High-order impulse approximation for calculating pulsed-field recombination

F. Robicheaux
Department of Physics, Auburn University, Auburn, Alabama 36849
and FOM Institute for Atomic and Molecular Physics, Kruislaan 407, 1098 SJ Amsterdam, The Netherlands
(Received 10 February 1999)

In a recent paper, Bensky *et al.* [Phys. Rev. Lett. **81**, 3112 (1998)] experimentally reattached an outgoing continuum electron to an ion using a pulsed electric field. Quantum and classical calculations are presented that illustrate the importance of various mechanisms for this reattachment process. The quantum calculations are based on a high-order impulse approximation. Both calculations support the idea that after an initial rapid dispersal, the bound part of the wave packet reforms after one Rydberg period; it continues to reform out to long times. A quantum calculation of the electron flux ejected from Ca Rydberg states in a static electric field suggests that classical calculations should not accurately describe pulsed-field recombination in the presence of a static field unless the atom is H or the fields are very weak; this observation agrees with experiment. [S1050-2947(99)06907-3]

PACS number(s): 32.60.+i, 32.80.Rm, 32.80.Fb

I. INTRODUCTION

There have been many recent experimental and theoretical investigations into the action of a half cycle pulse of an electric field on a Rydberg electron [1–25]. The pulsed electric fields can be used to control some aspects of the electron's motion and also can be used to probe the behavior of a Rydberg wave packet. The theoretical studies of this type of system have utilized both classical and fully quantum techniques. For low values of the principal quantum number, fully quantum techniques are used since the discrete nature of the bound levels is important. However, for high values of the principal quantum number, a purely classical approximation can accurately describe the behavior of these Rydberg systems kicked by a half cycle pulse since there are many nodes in the wave function (thus the correspondence principal is applicable). Often, the parameter being measured or calculated involves integration over a large part of the wave function; this strongly reduces interference effects which greatly increases the accuracy of purely classical calculations. Thus, classical calculations are accurate for much lower principal quantum numbers than might be expected.

Although classical methods should be accurate in many cases, quantum calculations should also be performed whenever possible. If both types of calculations are possible, this provides a double check on the theory since a quantum calculation does include interference effects which could be important, while classical calculations do not suffer from some of the problems of quantum calculations. For example, quantum calculations often suffer from convergence problems; basis sets become too large to allow the description of a particular experiment. This reasoning can also be reversed and leads to the implication that if there is substantial disagreement between the quantum and classical results then there may be interesting quantum effects governing the dynamics.

In this paper, the results of classical and fully quantum calculations are presented for pulsed field recombination of electrons and ions. Also, I describe the utilization of a substantially different technique for the quantum calculation than is usually employed: the action of the half cycle pulse on the electron is obtained by continuing the impulse approximation to high order until convergence is achieved [6]. Thus no basis functions are employed in the time propagation except for the Rydberg eigenstates in zero field. The coefficients of the eigenstates are obtained through numerical integration of two-dimensional functions. As a demonstration of the power of the method, the results presented in Sec. III A model the behavior of a wave packet with principal quantum number up to 180 and angular momentum as large as 150.

The qualitative effect of a half cycle pulse on a Rydberg electron has been discussed many times. If the pulse acts for a short enough time, the main effect is to give the electron a ''kick'' that changes its momentum by a fixed amount independent of its distance from the nucleus. For the part of the electron wave far from the nucleus, effects from the finite width of the pulse are thought to be small. The next order change arising from the finite width is the change in the electron's position due to the action of the pulse. A high-order impulse approximation can be developed, using the width of the pulse as the expansion parameter, and can be made to converge in certain cases. Each of the terms in the expansion has a physical meaning (e.g., the lowest order term is the impulse) which can serve as a guide to the applicability of impulse ideas to other systems.

Also, it will be obvious that if this series rapidly converges then very little information about the pulse is impressed on the wave function. This is analogous to the effect of a short-range potential in scattering problems. At low energy, very little information about the potential is obtained by scattering; roughly speaking only the depth and the range of the potential are important. For the action of a short electric-field pulse on an electron, only the change in the electron's momentum and the change in position due to the pulse are important; no other information about the pulse is important if the width is short enough.

II. HIGH-ORDER IMPULSE APPROXIMATION

The time-dependent Schrödinger equation for a Rydberg electron subjected to a pulsed electric field in the z direction has the form

$$i\frac{\partial\psi}{\partial t}=\left[\frac{p^2}{2}+V(\mathbf{r})-F(t)z\right]\psi \tag{1}$$

where $V(\mathbf{r})$ is a static potential; for the situation discussed in Sec. III A, the static potential has an asymptotic Coulomb form. (Atomic units are used throughout this paper.) The most typical method employed for solving this equation is an expansion of ψ in a time-independent basis. Calculating the time-dependent wave function thus reduces to a brute force numerical propagation of the coefficients of the basis set. The advantage of using this method is that all quantum effects are automatically included in the calculation. There are two disadvantages of this method. Often, the wave function cannot be converged with current computational resources. Also, it is often not possible to understand why the wave function behaves as it does which makes it difficult to extend the insight gained in one situation to other situations. For example, this method cannot be used for the experimental parameters in Ref. [25] since the size of the basis would be prohibitively large.

A completely different quantum method can be made to work for one of the experiments described in Ref. [25]. This method is essentially based on a transformation from the length to the acceleration gauge [6]. It can also be thought of as a systematic method for carrying the impulse approximation to higher order. This method only works when the duration of the electric field is small. To be specific, we suppose that the electric-field pulse is essentially zero except for the range of time $t_1<t<t_2$ and that the pulse duration $T\equiv t_2-t_1$ is small with the restriction on T given below.

The derivation of the wave function after the electric field is given in the Appendix. During and just after the pulse, the wave function is given by

$$\Psi(\mathbf{r},t)\simeq\exp[-i\varphi(t)]\exp[i\Delta p_z(t)z]\times\exp[-i\Delta z(t)p]\exp[-i\delta(\mathbf{r},t)]\psi_0(\mathbf{r},t), \tag{2}$$

where ψ_0 is the wave function if there were no electric-field pulse and

$$\Delta p_z(t)=\int_{-\infty}^{t}F(t')dt', \tag{3}$$

$$\varphi(t)=\int_{-\infty}^{t}\Delta p_z^2(t')dt'/2, \tag{4}$$

$$\Delta z(t)=\int_{-\infty}^{t}\Delta p_z(t')dt', \tag{5}$$

$$\delta(\mathbf{r},t)=(\partial V(\mathbf{r})/\partial z)\int_{-\infty}^{t}\Delta z(t')dt'. \tag{6}$$

In the exponentials in Eq. (2), p_z is the momentum operator in the z direction $(-i\partial/\partial z)$ and z is the position in the z direction. There is a physical interpretation to each of the exponentials in Eq. (2). The exponential with the Δp_z gives the change in the momentum due to the impulse from the pulsed electric field. The exponential with the Δz gives the change in the position due to the pulsed electric field. The term with $\varphi(t)$ gives the change in phase due to the temporary change in energy during the pulse; this term has no physical effect on the wave function since it only gives an overall phase change after the pulse. The term with the $\delta(\mathbf{r},t)$ gives the change in the change in momentum due to the acceleration of the electron from the static potential during the electric-field pulse; this is the only term in Eq. (2) that depends on the position of the electron.

The size of the different terms can be estimated from the maximum of the electric-field pulse $F_{\max}$ and the duration of the pulse, T. The impulse $\Delta p_z\sim F_{\max}T$. The change in position due to the impulse is $\Delta z\sim F_{\max}T^2$. The change in the change in momentum due to the Coulomb field is $\sim F_{\max}T^3/r^2$. The convergence and applicability of the higher-order impulse approximation depends on the size of the terms relative to the parameters being measured.

The exponential with δ must be included when the change in δ across the nonzero part of ψ_0 is greater than ~ 1. For example, reasonable accuracy can be obtained when only a small fraction of the wave function is within $\sqrt{F_{\max}T^3}$ of the nucleus. Whether or not it is necessary to include the exponential with Δz is a difficult question that depends on the situation being investigated. In some experiments, the change in energy due to the action of the pulsed field is the only important parameter; for this situation, one can estimate the change in potential energy due to the Δz term and compare to the change in kinetic energy due to the impulse. In some experiments, the final-state distribution is important and can sensitively depend on whether or not Δz is included.

To gain some intuition about the sizes of terms for a realistic experiment, I used the parameters from Ref. [25]. For $F_{\max}=2100$ V/cm$=4.1\times10^{-7}$ a.u. and $T=1$ ps$=4.1\times10^4$ a.u., the impulse is 0.017 a.u., the change in position is 700 a.u., and the change in the momentum is $\sim 2.8\times10^7/r^2$. For these parameters, the higher-order impulse approximation will work well if the electron is further than 5300 a.u. from the nucleus. For the experiments in Ref. [25], the effect from δ is negligibly small but the effect from the change in position Δz is noticeable.

If this method converges, it implies that very little information about the pulsed electric field is impressed on the wave function. For example, suppose that the third-order term $\delta(\mathbf{r},t)$ is negligible. For this case, the only two properties of the pulsed electric field that affect the wave function are the impulse Δp_z and the change in position Δz: the only important aspects of the field is its time integral and the double integral

$$\Delta z(t)=\int_{-\infty}^{t}dt'\int_{-\infty}^{t'}dt''F(t''). \tag{7}$$

This is analogous to low-energy scattering from a short-range potential where the scattering cross section only de-

pends on the strength and the range of the potential. When the impulse approximation is applicable, the final results do not depend on the details of the pulse but only depend on two parameters: $\Delta p_z(t_2)$ and $\Delta z(t_2)$.

The wave function at any time after the electric-field pulse ($t > t_2$) may be obtained by projecting the wave function onto the eigenstates of the static potential. Thus, all of the numerical effort is condensed into numerically evaluating integrals. The eigenstates are defined in the usual way

$$\left[\frac{p^2}{2} + V(\mathbf{r})\right]\psi_n(\mathbf{r}) = E_n\psi_n(\mathbf{r}), \tag{8}$$

where ψ_n are the orthonormal eigenstates and E_n are the eigenenergies. The wave function at any time after the pulse is given by

$$\Psi(\mathbf{r},t) = \sum_n \psi_n(\mathbf{r}) C_n \exp[-iE_n(t-t_2)], \tag{9}$$

where the time-independent coefficients are given by

$$C_n = \int \psi_n^*(\mathbf{r})\Psi(\mathbf{r},t_2)d\mathbf{r}. \tag{10}$$

The integrations can be quite time consuming but do not use much memory.

This method can be implemented in several ways that incorporate different levels of approximation and insight. For example, if the integrals in Eqs. (9) and (10) are performed using WKB wave functions and the stationary phase approximation, then a semiclassical approximation results which connects the evolution of the wave function into different regions of space with classical trajectories. At the most accurate level, the eigenstates and wave functions are obtained exactly with the numerical integrations performed using small radial step sizes and high-order integration techniques. In the current implementation, the radial eigenstates are calculated exactly for zero and one nodes in the radial direction; for a higher number of nodes, a uniform WKB approximation [26] based on the Milne method was used with the Airy function from each turning point being matched at the midpoint of the classically allowed region.

III. RESULTS

The ideas of the previous section were used to analyze the two experimental arrangements described in Ref. [25].

A. Pulsed-field recombination: $F_{\text{static}} = 0$

In Ref. [25], an interesting experimental arrangement was realized. Low-energy continuum electrons were produced through the interaction of a pulsed laser ($\sim$1.5 ps width) with Ca atoms in the $4s4p\ ^1P_1^o$ state. This creates a radially outward moving shell of electron probability. Thus an outgoing electron at the point $(x,y,z) = r(\cos\phi\sin\theta, \sin\phi\sin\theta, \cos\theta)$ has momentum $p_x = p\cos\phi\sin\theta$, $p_y = p\sin\phi\sin\theta$, and $p_z = p\cos\theta$. After a short delay, a half cycle pulse of electric field ($\sim$1 ps width) interacted with the outgoing electron. This electric-field pulse affects the motion of the electron; the main effect is to give a momentum change to the electron: $\hat{z}\Delta p_z$. After the pulse, the electron's momentum is $(p_x, p_y, p_z + \Delta p_z)$ where (p_x, p_y, p_z) is the electron's momentum before the pulse. Depending on the strength of the half cycle pulse and the delay between the laser pulse and electric-field pulse, part of the continuum wave can be stopped; thus changing part of the outgoing continuum wave into a bound-state Rydberg wave packet. An interesting aspect of this process is that only a small angular extent of the outgoing wave packet will become bound when the impulse given to the electron exactly cancels the electron's original momentum on the z axis.

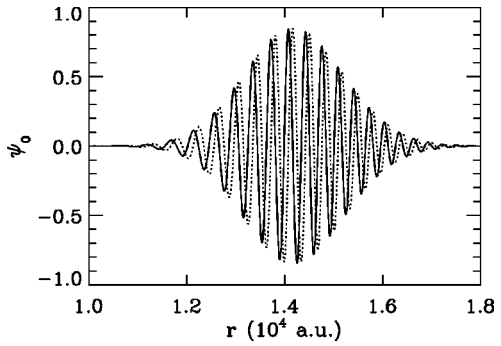

FIG. 1. The real (solid line) and imaginary (dotted line) part of the unperturbed radial wave function is plotted at a time just after the half cycle pulse. The angular momentum is 2 and the z component of the angular momentum is 0.

Fully quantum basis set calculations are not possible for the parameters used in the experiment. However, the situation explored in the experiment was ideal for the use of the higher-order impulse approximation [6]. No part of the electron wave is near the nucleus. The parameters used in the calculation were: maximum field strength of 2103 V/cm, the electric-field pulse of duration 1 ps at full width at half maximum (FWHM), the laser pulse excited the electron only to outgoing d waves with the z component of angular momentum equal to zero, a central energy of 20 cm^{-1} above the ionization threshold, width of the laser pulse of 1.5 ps at FWHM, and the time of the maximum field strength was 13.2 ps after the laser excitation. For the Gaussian pulse used in the calculation, the impulse $\Delta p_z = 0.018$ a.u. and the change in position $\Delta z = 1116$ a.u.

The results from the high-order impulse calculation were compared to classical calculations. For the classical calculations, a Monte Carlo distribution of 320 000 trajectories was used. The distribution was chosen to simulate all important aspects of the quantum wave packet. The time of launch of the electron had a distribution in proportion to the time-dependent intensity of the laser pulse. The trajectories had a distribution in energy proportional to the quantum energy distribution. And the trajectories were launched with zero angular momentum but with an angular distribution matching the quantum d-wave angular distribution; the electron's initial angular momentum had no noticeable effect on the classical dynamics because the electron was extremely far from the nucleus during the electric-field pulse.

In Fig. 1, the real and imaginary part of the unperturbed radial wave function is plotted at time t_2 to show the position and wave length of the electron. All of the electron probabil-

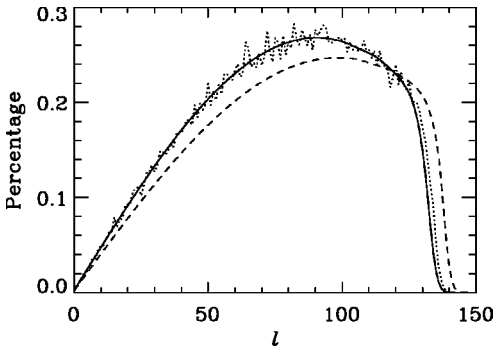

FIG. 2. The angular momentum distribution after the half cycle pulse. The dotted line is the classical distribution. The dashed line is the lowest order impulse approximation which only includes the change in momentum due to the pulse. The solid line is the second-order impulse approximation which includes the change in momentum and the change in position due to the pulse. The third-order approximation is indistinguishable from the second-order approximation in this figure.

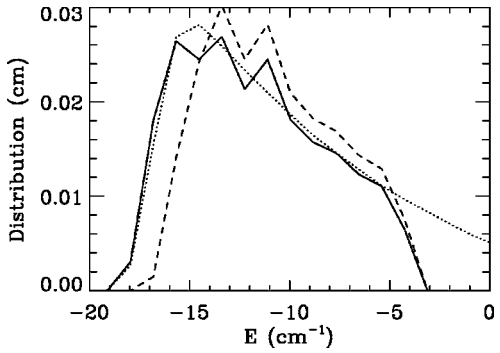

FIG. 3. Same as Fig. 2 but for the energy distribution.

ity is further than 10^4 a.u. from the nucleus and the wave length of the electron is roughly 350 a.u. The highest-order correction term δ is nowhere larger than 0.3 and it was found that convergence was achieved after including Δz.

The classical and quantum angular momentum distribution after the electric-field pulse are plotted in Fig. 2; the distribution is only for the part of the packet with energy less than 3.4 cm^{-1} below threshold. The quantum distribution is plotted for the first-order impulse approximation, $\Delta z=0$ and $\delta=0$, the second-order impulse approximation, $\delta=0$, and the third-order impulse approximation. There are a number of important features of the distribution that should be noticed. The first feature is the rapid convergence of the impulse approximation with order. The main shape is reproduced with the lowest order impulse approximation; the second-order impulse approximation gives an essentially exact result even though it only includes the change in momentum and change in position due to the electric-field pulse. Another interesting feature is that less than 0.04% of the electron probability is in angular momentum less than or equal to 3; this means that the behavior of the wave after the electric-field pulse will be nearly independent of the atom since it is only the $\ell \leqslant 3$ partial waves that have nonzero quantum defect. A final interesting feature is the sharp cutoff of the probability near angular momentum of 135 which arises from the physical impossibility of having angular momentum larger than $r_{\max}p_{\max}$. The lowest order impulse approximation extends further in angular momentum because the bound part of the packet is pushed back towards the nucleus in the higher-order approximation which slightly decreases $r_{\max}$ and therefore the maximum angular momentum.

In Fig. 3, the quantum and classical energy distributions are plotted. As in Fig. 2, the first- through third-order impulse approximations are plotted for the quantum calculation to show the convergence of the wave function. The quantum distributions are restricted to energies less than 3.4 cm^{-1} below the threshold in order to model the recombined part of the wave packet. Notice how the sharp rise of the quantum distribution depends on the order of the impulse approximation. The edge of the rise decreases in energy in going from first to second order. The difference between these calculations is the inclusion of the Δz term. The edge of the rise decreases in energy when including the Δz term because this part of the energy distribution is from the fraction of the wave packet that is opposed by the half cycle pulse; this part of the packet loses energy because p_z is decreased and it also loses energy in second order because that part of the packet is moved back towards the nucleus.

One of the interesting features of Ref. [25] was a discussion of the behavior of the bound part of the packet. In Fig. 4 the quantum density is plotted for the part of the wave function with energy less than 3.4 cm^{-1} below the threshold and in Fig. 5 the corresponding classical density is plotted. Note the small angular extent of the packet and also the rapid dispersal of the packet at short times. (Because of the small angular features, both the quantum and classical densities at r, $\cos\theta$ is integrated over the angular step.) The small angular extent just after the pulse can occur because of the large distribution of angular momenta shown in Fig. 2. At later times, the packet reforms very near the position it was originally formed. The time at which it reforms can be estimated from its original radial position, $\sim 1.3\times 10^4$ a.u. This distance corresponds to a principal quantum number, $r\sim 2n^2$, of roughly 80; the Rydberg period corresponding to this principal quantum number is roughly 80 ps. It was found [25] that the packet reformed after one Rydberg period.

A striking feature of the probability distribution is the good agreement between the classical and quantum calculations. Even quite subtle and strange features are reproduced. For example, the band of probability near $\cos\theta=0$ is visible in both the quantum and classical 48 ps graph; also the details of the triangular structure near $\cos\theta=1$ is visible in both the quantum and classical 120 ps graph. The only feature not reproduced by the classical calculation is some interference patterns; on the scale of these graphs the only visible occurrence is in the 24 ps graph near $\cos\theta=0.5$ and $r=1.5\times 10^4$ a.u. This suggests that simple semiclassical calculations that included interference would be able to account for all of the features of the quantum calculation.

Figures 4 and 5 verify the striking behavior of the bound part of the wave packet. In fact, calculations showed the wave packet continues to reform even out to very long times. This shows that there is plenty of time after the initial electric-field pulse to perform further manipulations on the atom. For example, another electric-field pulse could kick the electron to the side and launch it in a circular orbit or another laser pulse could launch the inner electron to a

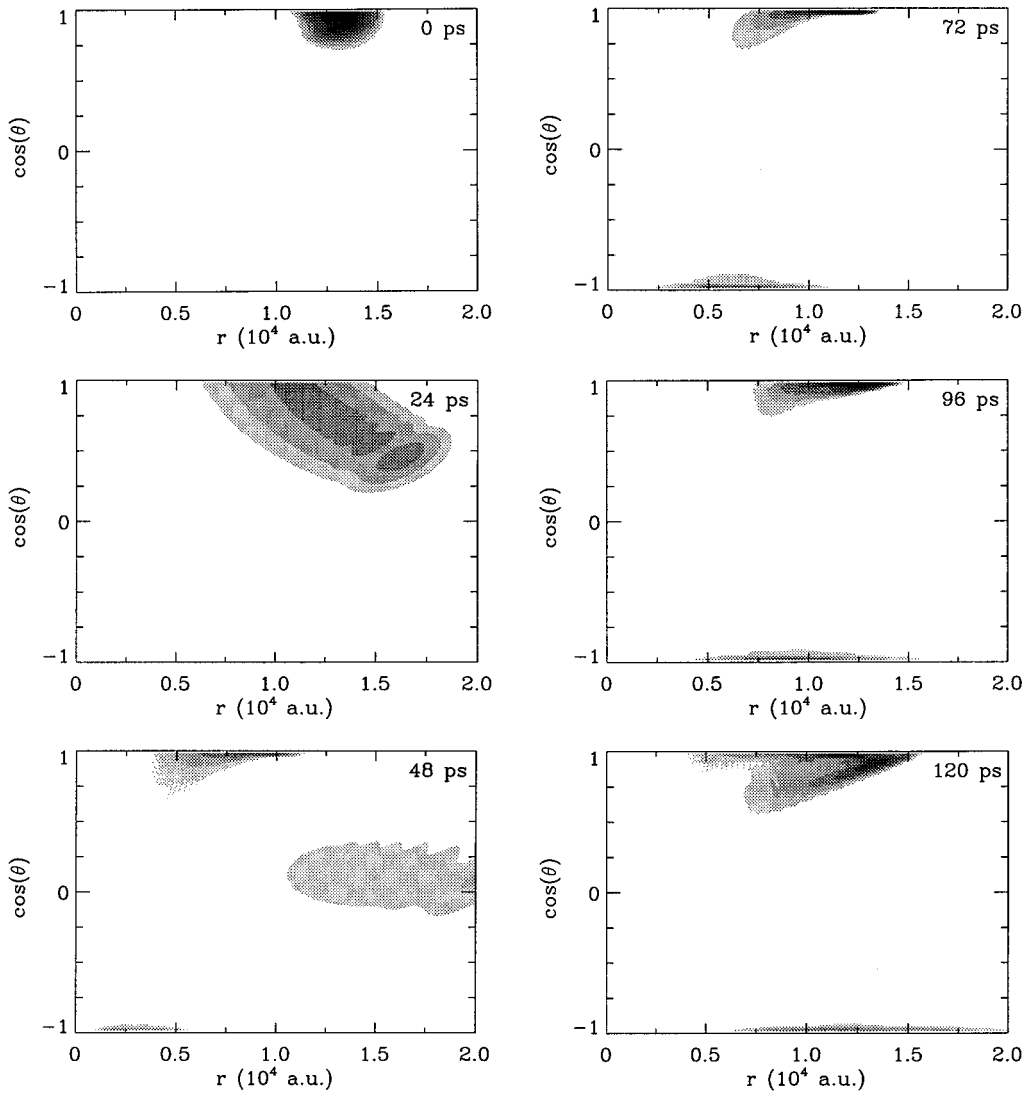

FIG. 4. After the half cycle pulse, the quantum spatial distribution for the part of the packet at energies less than 3.4 cm^{-1} below the ionization threshold. The times in the upper right corner are measured from just after the half cycle pulse. The packet quickly disperses but reforms near times of 72 ps. The original angular extent is very small because there is a large angular momentum distribution.

Rydberg wave packet thus making a double Rydberg wave packet.

B. Pulsed-field recombination: $F_{\text{static}} \neq 0$

A second series of experiments in Ref. [25] gave extremely striking results considered from a general perspective. In these experiments, a Rydberg wave packet in Ca was initiated by a pulsed laser but with Ca in a static electric field of 212 V/cm. The wave packet was created at an energy such that the electron could not escape in zero field but could escape with the field on. For the results presented, the central energy of the packet corresponded to the zero-field position of $n=42$ states. After a time delay, a pulsed electric field of $\sim$2700 V/cm and 1 ps duration was applied. The probability for causing the electron to remain attached to the atom was measured; the electron will remain attached to the ion if the Rydberg electron has less energy than $-2\sqrt{F}$ relative to the zero-field threshold after the pulsed electric field.

The surprising feature of this experiment was that a classical simulation only produced qualitative agreement and this qualitative agreement only extended for 20–30 ps after the laser excitation. Why do the classical calculations reproduce the quantum calculations so well for zero static field but give only marginal agreement for nonzero static field? All indications are that this experiment should be very accurately simulated by a classical calculation since the measured quantity is the probability for the electron to have energy less than $-2\sqrt{F}$ after the electric-field pulse. This quantity involves an enormous amount of averaging and thus one does not expect any quantum effects to survive.

The key to explaining the discrepancy rests with the behavior of the Rydberg wave packet from the time it is excited to the time the electric-field pulse is applied. Just after the laser excitation, part of the wave packet moves down field and directly leaves the atom while part of the packet moves up field and is temporarily trapped near the atom. If the atom is hydrogen, then the temporarily bound part of the packet is trapped near the atom for a very long time. This is because the Hamiltonian for H in a static field is separable; thus, the trapped part of the packet can only leave the atom by tun-

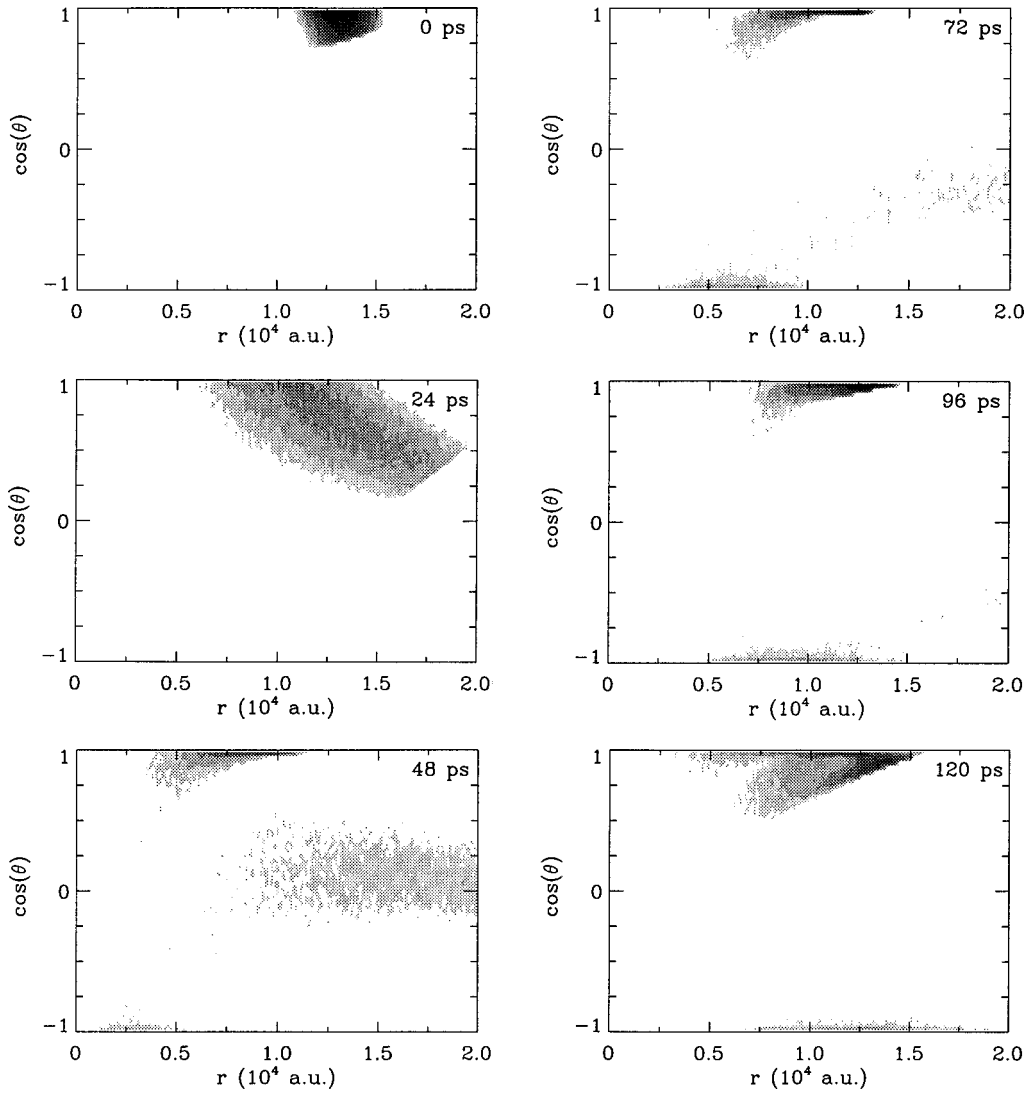

FIG. 5. Same as Fig. 4 but the classical spatial distribution.

neling which is a relatively slow process. However for Ca, the trapped part of the packet can also escape by elastically scattering off of the nonhydrogenic potential generated by the core electrons and move down field. The speed with which the packet can scatter down field depends on the field strength and on the n states excited and on the size of the quantum defects.

In Fig. 6, the fraction of the wave packet left on the atom is plotted as a function of time after the laser excitation; there is roughly a 10 ps delay between when the electron begins moving in the down potential direction and when it is counted as having left the atom. This fraction can be calculated using the time-dependent flux of electrons ejected from the atom. Using $I(t)$ to denote the time-dependent flux of ejected electrons, the fraction of the wave packet left on the atom is

$$f(t)=\int_t^\infty I(t')dt' \Big/ \int_{-\infty}^{\infty} I(t')dt'. \tag{11}$$

Notice that roughly half of the packet is excited to the temporarily bound region of space. However, during the course of the experiment most of the originally bound part of the packet subsequently escapes. Only 20% is left on the atom after 120 ps. Roughly 30 ps after the initial excitation, the fraction bound to the atom drops from roughly 50% to below

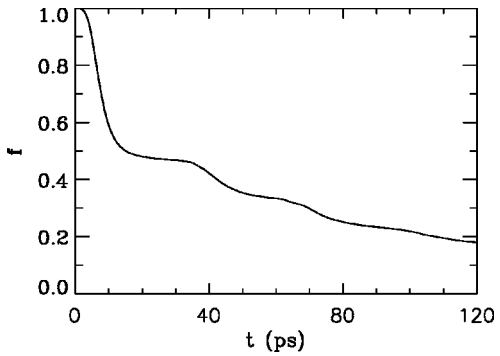

FIG. 6. The fraction of the probability distribution still in the bound region near the Ca atom is plotted versus the time after the excitation. There is a 10 ps time shift between when the electron begins moving in the down potential direction and when it is counted as having left the atom. Note that originally 50% of the probability is bound to the atom, but only 20% remains after 120 ps.

40% which means that after a short time over 20% of the electron probability that was initially bound to the atom has left.

There is a further effect that skews the distribution in the bound region. This is the effect arising from the large energy distribution in the original laser excitation. This energy distribution extends from just above the classical ionization threshold in the field to energies just below the ionization threshold in zero field. The difficulty with such a broad energy distribution is that near the ionization threshold in the field it is difficult for the electron to scatter in the down field direction and leave the atom. However, near the ionization threshold in zero field, it is very easy for the electron to scatter in the down potential direction and leave. Thus, the higher energy components rapidly scatter and leave the atom while the lower energy components are bound for a longer time; the energy distribution shifts to lower energy with time. This introduces a large uncertainty in how the half cycle pulse will affect the wave packet because the long time tail of the pulse can cause the small change in energy needed to cause the electron to lose enough energy to become bound.

The explanation of the discrepancy between the experiment and the classical simulation appears to be founded on a relatively large quantum effect: the scattering of the electron wave from the non-Coulombic potential arising from the core electrons. This effect can be decreased by using an atom with a smaller core (e.g., Li) and can be eliminated by using hydrogen. It can also be decreased by using smaller static fields and going to higher energy; as the principal quantum number increases, the fraction of angular momenta that have nonzero quantum defects decreases which reduces the amount of scattering.

The contribution of the non-Coulombic core potential to the dynamics was inferred by examining the scattering of the electron into the unbound region of space. However, it must be remembered that part of the scattered wave will remain in the bound region of space thus changing the form of the bound probability distribution. This is why the experimental results and classical simulation only qualitatively agree for a short time.

IV. CONCLUSIONS

A higher-order impulse approximation has been applied to the calculation of quantum wave packets affected by a pulsed electric field. A physical interpretation for the first three orders was given which allows an understanding of even fine details of the electron probability distribution. Results for parameters used in Ref. [25] were presented; this approximation allowed the calculation to correctly include the behavior of angular momenta as high as 150 and principal quantum numbers as high as 180. Also, the discrepancy between the experimental results and classical simulation in Ref. [25] was analyzed and shown to result from a quantum property of the non-Coulombic potential.

ACKNOWLEDGMENTS

F.R. is supported by the NSF. This work is part of the research program of the ''Stichting voor Fundamenteel Onderzoek der Materie (FOM),'' which is financially supported by the ''Nederlandse organisatie voor Wetenschappelijke Onderzoek (NWO).''

APPENDIX

The wave function for the higher-order impulse approximation is obtained by a series of gauge transformations [6]. The transformation from length to velocity gauge gives

$$\Psi(\mathbf{r},t)=\exp[i\Delta p_z(t)z]\overline{\psi}(\mathbf{r},t), \tag{A1}$$

where the $\Delta p_z(t)=\int_{-\infty}^{t}F(t')dt'$ is the classical change in momentum of a free electron subjected to a pulsed electric field; for $t>t_2$, Δp_z is a constant and is the impulse given to a free electron by the pulsed field. The function $\overline{\psi}$ is the solution of the velocity gauge Schrödinger equation

$$i\frac{\partial\overline{\psi}}{\partial t}=\left[\frac{p^2}{2}+\Delta p_z(t)p_z+\frac{\Delta p_z^2(t)}{2}+V(\mathbf{r})\right]\overline{\psi}. \tag{A2}$$

The time-dependent function $\Delta p_z^2(t)/2$ only contributes an overall phase and has no effect on any observable. The transformation from velocity gauge to acceleration gauge gives

$$\overline{\psi}(\mathbf{r},t)=\exp[-i\varphi(t)]\exp[-i\Delta z(t)p_z]\tilde{\psi}(\mathbf{r},t), \tag{A3}$$

where the $\Delta z(t)=\int_{-\infty}^{t}\Delta p_z(t')dt'$ is the change in position of a free electron due to the pulsed electric field and the time-dependent phase $\varphi(t)=\int_{-\infty}^{t}\Delta p_z^2(t')/2dt'$ is irrelevant. The $\tilde{\psi}$ wave function is the solution of the acceleration gauge Schrödinger equation

$$i\frac{\partial\tilde{\psi}}{\partial t}=\left[\frac{p^2}{2}+\exp[i\Delta z(t)p_z]V(\mathbf{r})\exp[-i\Delta z(t)p_z]\right]\tilde{\psi}. \tag{A4}$$

The next order correction can be obtained by expanding the exponentials to first order in $\Delta z(t)$. This gives the approximate equation

$$i\frac{\partial\tilde{\psi}}{\partial t}=\left[\frac{p^2}{2}+V(\mathbf{r})+\Delta z(t)\frac{\partial V}{\partial z}\right]\tilde{\psi}. \tag{A5}$$

This process can be continued indefinitely; however, for the case discussed in this paper, convergence is achieved at this order. The wave function can be well approximated by

$$\tilde{\psi}\simeq\exp[-i\delta(\mathbf{r},t)]\psi_0(\mathbf{r},t), \tag{A6}$$

where $\delta(\mathbf{r},t)=\int_{-\infty}^{t}\Delta z(t')dt'\partial V/\partial z$ and ψ_0 is the wave function without any electric-field pulse.

[1] R.R. Jones, D. You, and P.H. Bucksbaum, Phys. Rev. Lett. **70**, 1236 (1993).
[2] C.O. Reinhold, M. Melles, and J. Burgdörfer, Phys. Rev. Lett. **70**, 4026 (1993).
[3] D. You, R.R. Jones, D.R. Dykaar, and P.H. Bucksbaum, Opt. Lett. **18**, 290 (1994).
[4] C.O. Reinhold, H. Shao, and J. Burgdorfer, J. Phys. B **27**, L469 (1994).
[5] K.J. LaGattuta and P.B. Lerner, Phys. Rev. A **49**, R1547 (1994).
[6] P. Krstic and Y. Hahn, Phys. Rev. A **50**, 4629 (1994).
[7] C.O. Reinhold, J. Burgdörfer, R.R. Jones, C. Raman, and P.H. Bucksbaum, J. Phys. B **28**, L457 (1995).
[8] R.R. Jones, N.E. Tielking, D. You, C.S. Raman, and P.H. Bucksbaum, Phys. Rev. A **51**, 3370 (1995).
[9] N.E. Tielking, T.J. Bensky, and R.R. Jones, Phys. Rev. A **51**, 3370 (1995).
[10] N.E. Tielking and R.R. Jones, Phys. Rev. A **52**, 1371 (1995).
[11] G.M. Lankhuijzen and L.D. Noordam, Phys. Rev. Lett. **74**, 355 (1995).
[12] A. Bugacov, B. Piraux, M. Pont, and R. Shakeshaft, Phys. Rev. A **51**, 1490 (1995); **51**, 4877 (1995).
[13] C. Raman, C.W.S. Conover, C.I. Sukenik, and P.H. Bucksbaum, Phys. Rev. Lett. **76**, 2436 (1996).
[14] C.O. Reinhold, M. Melles, H. Shao, and J. Burgdörfer, J. Phys. B **26**, L659 (1993); **29**, 377 (1996).
[15] M.T. Frey, F.B. Dunning, C.O. Reinhold, and J. Burgdörfer, Phys. Rev. A **53**, R2929 (1996).
[16] R.R. Jones, Phys. Rev. Lett. **76**, 3927 (1996).
[17] F. Robicheaux, Phys. Rev. A **56**, R3358 (1997).
[18] R. Gebarowski, J. Phys. B **30**, 2143 (1997).
[19] C. Raman, T.C. Weinacht, and P.H. Bucksbaum, Phys. Rev. A **55**, R3995 (1997).
[20] T.F. Jiang and C.D. Lin, Phys. Rev. A **55**, 2172 (1997).
[21] C.W.S. Conover and J.H. Rentz, Phys. Rev. A **55**, 3787 (1997).
[22] P. Kristensen, G.M. Lankhuijzen, and L.D. Noordam, J. Phys. B **30**, 1481 (1997).
[23] R.B. Vrijen, G.M. Lankhuijzen, and L.D. Noordam, Phys. Rev. Lett. **79**, 617 (1997).
[24] S. Yoshida, C.O. Reinhold, J. Burgdörfer, B.E. Tannian, R.A. Popple, and F.B. Dunning, Phys. Rev. A **58**, 2229 (1998).
[25] T.J. Bensky, M.B. Campbell, and R.R. Jones, Phys. Rev. Lett. **81**, 3112 (1998).
[26] F. Robicheaux, U. Fano, M. Cavagnero, and D.A. Harmin, Phys. Rev. A **35**, 3619 (1987).